Pure and Mixed Phase Bi2O3 Thin Films Obtained by Metal Organic Chemical Vapor Deposition

5 AUTHORS, INCLUDING:

Davide Barreca
National Research Council, Padova
289 PUBLICATIONS   **4,290** CITATIONS

SEE PROFILE

Gian Andrea Rizzi
University of Padova
87 PUBLICATIONS   **1,300** CITATIONS

SEE PROFILE

[11] A. D. Berry, R. T. Holm, M. Fatemi, D. K. Gaskill, *J. Mater. Res.* **1990**, 5, 1169.

[12] M. Miyajima, R. Muhammet, M. Okada, *J. Chem. Soc. Jpn.* **1991**, 10, 1373.

[13] G. A. Neuman, *Eur. Patent No. 0 353 461 B1*, **1993**.

Pure and Mixed Phase Bi₂O₃ Thin Films Obtained by Metal Organic Chemical Vapor Deposition

By *Giuliano Bandoli, Davide Barreca, Enrico Brescacin, Gian A. Rizzi*, and *Eugenio Tondello**

Bismuth oxides have important catalytic properties in oxidation reactions such as ammoxidation for the synthesis of acrylonitrile from propylene, oxygen, and ammonia. Such powerful catalytic activity appears to be correlated with the existence of variable oxidation states of bismuth and with the high oxygen mobility on the surface. Bismuth(III) oxide also has many different technical applications such as Schottky barrier solar cells, optical coatings, and dielectric materials in metal insulator semiconductor capacitors.[1] Therefore, taking into account both the reactivity of the surface and the electrical properties, bismuth oxide in the form of films or thin films can also find important applications in gas sensor devices.

However, since the phase and morphology of the films strongly affect the functional properties, we carried out the synthesis of pure Bi₂O₃ thin films with the aim of studying the influence of the substrate and of the process parameters on the growth modality and structure of the coatings.

The Bi–O system is rather complicated and can have four different main crystalline phases, usually indicated with the letters α, β, γ, and δ. Only the α- and β-Bi₂O₃ phases are well characterized, since they are stable at room temperature, while the γ and δ phases can be obtained only at high temperatures ($T > 1003$ K for δ and $T > 908$ K for γ). Each of these phases has different electrical properties, ranging from a typical electronic conduction behavior in the α phase to a perfectly ionic conduction mechanism in the δ phase.[2]

Because of the different electrical properties found in each of the Bi₂O₃ phases it is clear that a possible use of bismuth oxide films in gas sensing devices is connected with the possibility of controlling the stoichiometry and the morphology in the deposition procedures.

Thin films can be prepared by different techniques.[1] Thermal evaporation of bismuth oxide is rather difficult because molten Bi₂O₃ attacks almost all crucible materials except platinum. Another method is the thermal oxidation of Bi films, but the samples obtained in such a way are usually a mixture of different phases. Reactive evaporation of Bi and activated reactive evaporation have been successfully used to prepare single-phase Bi₂O₃ films.[1] Good quality films can be prepared by reactive sputtering of Bi in an O₂ atmosphere. The high temperature δ phase coexists with a glass phase in Bi₂O₃–SiO₂ films prepared by the rapid quenching technique.[3] Metal-organic chemical vapor deposition has recently been used to deposit Bi₂O₃ films[4] but the α and β phases have never been obtained pure.

It is well known that the morphology, crystallinity, and purity of films prepared by MOCVD are strongly dependent not only on the precursor and substrates used, but also on the deposition parameters such as flow rate, pressure, and temperature. Thus MOCVD appears to be an ideal technique to deposit Bi₂O₃ films with high purity on different substrates and to control their crystal phase.

To this end, Bi(Ph)₃ is used as precursor and different deposition conditions are used to obtain pure α, β or mixed α + β phase Bi₂O₃ thin films on surface-oxidized Si(100) and Al₂O₃ as substrates. While Al₂O₃ is commonly used in commercial devices, SiO₂/Si(100) will presumably be used in the near future because it offers the possibility of having both the sensor and the control electronics in the same Si chip. The films are characterized by XPS and XRD and their surface morphology is analyzed by atomic force microscopy. Moreover, also FTIR spectroscopy is used as a tool for an easy and fast preliminary identification of the phase composition of the deposited films, following recent IR and Raman applications in transition metal oxides and complex oxide systems such as bismuth molybdates.[5]

Several depositions were performed on surface oxidized Si(100) (n-type) and Al₂O₃ using different process conditions. On surface oxidized Si(100), with a total pressure of 6 mbar, pure β phase is obtained when using low gas flow rates. The α + β phases were obtained at higher flow rates. The results and the corresponding deposition parameters are summarized in Tables 1 and 2.

Table 1. Growth conditions for samples deposited on SiO₂/Si(100).

Sample/Phase	Total pressure (mbar)	Flow rate (sccm)
1/β	6	50
2/α + β	6	100
3/α + β	6	200
4/α + β	12	50
5/α	12	100
6/β	12	200

Precursor temperature = 110 °C; precursor vapor pressure (110 °C) = 0.04 mbar [16].

Crystalline phases of the films were determined by XRD analysis. FTIR analysis of the films deposited on SiO₂/Si(100) proved to be useful since the different crystal struc-

[*] Prof. E. Tondello, Dr. D. Barreca, Dr. E. Brescacin, Dr. G. A. Rizzi
Centro di Studio sulla Stabilità e Reattività
dei Composti di Coordinazione del CNR
Dipartimento di Chimica Inorganica, Metallorganica ed Analitica
Università di Padova
Via Marzolo, 1, I-35131 Padova (Italy)

Prof. G. Bandoli
Dipartimento di Scienze Farmaceutiche
Università di Padova
Via Marzolo, 5, I-35131 Padova (Italy)

Table 2. Growth conditions for samples deposited on Al_2O_3.

Sample/phase:	7/α	8/β
Precursor temperature (°C)	120	90
Substrate temperature (°C)	420	420
Total pressure (mbar)	6	6
O_2 flow rate (sccm)	50	400

Precursor vapor pressure (90 °C) = 0.008 mbar; precursor vapor pressure (120 °C) = 0.08 mbar [16].

tures of α and β phases make significant differences in the IR patterns. However, to our knowledge very few examples of Bi_2O_3 IR spectra have been reported in the literature,[6] and no data about the β phase are available. Therefore, the mid-IR spectra of freshly prepared α- and β-Bi_2O_3 powder samples that had previously been characterized by XRD were recorded. In Figure 1 the diffuse reflectance IR spec-
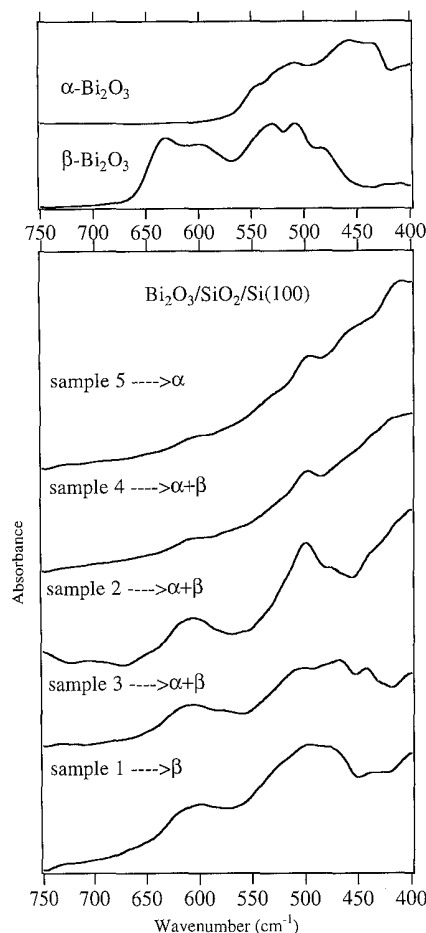

Fig. 1. Comparison of IR spectra of Bi_2O_3 films deposited on SiO_2/Si(100) with IR spectra of powder α- and β-Bi_2O_3 phases.

tra of the powders are reported with the IR spectra of the films deposited on oxidized Si(100). The spectrum of the β phase shows four bands at 631 (m), 597 (m), 530 (s), and 508 (s) and a shoulder at 482 cm^{-1}. No strong absorptions are found in the 450–400 cm^{-1} region. In contrast, the IR spectrum of the α phase shows a strong absorption cen-

tered at 442 cm^{-1} with shoulders at 512 and 550 cm^{-1}. No bands are found above 600 cm^{-1}. Therefore the bands at 631 and 597 cm^{-1} can be used to easily identify the presence of the β phase in the films.

The XRD patterns of samples 1 and 6 (not reported in the figure) exactly match with the diffractogram of β-Bi_2O_3[1,7,8] with strong peaks at $2\Theta = 28°$ and $58°$ and a weak peak at $2\Theta = 24°$ corresponding respectively to reflections (201), (402), and (210). Therefore both samples seem to have a preferential orientation of the crystallites along the direction perpendicular to (201) planes. The IR spectra of both samples, as expected, show an unresolved band at about 600 cm^{-1} and a stronger absorption centered at about 490 cm^{-1} (see Fig. 1). An imperfect background subtraction which leaves residual absorptions of SiO_2 at 610 cm^{-1} is responsible for the unresolved structure of the 600 cm^{-1} band. The XRD pattern of sample 5 is characteristic of α-Bi_2O_3[1,9] with the most intense peaks at $2\Theta = 27.5°$ (shoulders at 27° and 28.2°), 33.3°, and 46.6°. The corresponding IR spectrum does not show bands between 600 and 650 cm^{-1} but presents a strong absorption at 410 cm^{-1} and a shoulder at 497 cm^{-1}. In all cases (samples 1, 5, and 6) the FTIR data are in agreement with the X-ray diffractograms. Samples 2 and 3 show an XRD pattern where reflections from both α and β phases are present and correspondingly the IR spectra appear as a superposition of bands due to α- and β-Bi_2O_3 (see Fig. 1): α and β phases are present in these samples in comparable amounts. The IR spectrum of sample 4 resembles very well the one of sample 5; however, very weak absorptions between 590 and 620 cm^{-1} are present and a less pronounced shoulder is found at about 450 cm^{-1}. As expected, the XRD pattern contains reflections due to both phases, even if those corresponding to the β phase are much weaker. Therefore sample 4 is mainly formed by α-Bi_2O_3 with traces of β-Bi_2O_3.

When the film deposition is carried out on Al_2O_3 using the same parameters of sample 1 (pure β phase) and a precursor temperature of 120°C the XRD pattern obtained corresponds to α-Bi_2O_3. The β phase can be obtained on Al_2O_3 in the conditions summarized in Table 2.

The composition and purity of the films were studied by XPS. All the films show a lower oxygen content with respect to the value expected for a Bi_2O_3 stoichiometry. The obtained O/Bi ratios of the as-grown samples range from 1.2, in the case of the β phase, to 1.4 in the case of the α phase. It is worth to note that, according to the XRD data, the β phase is actually formulated as β-Bi_2O_{3-x} because of the oxygen vacancies found in the lattice.[7] A further annealing of the samples in air at 400 °C does not cause significant changes to the O/Bi ratios. The binding energy values for the Bi 4f and O 2p peaks, reported in Table 3, are in good agreement with the values reported in the literature,[10] even if it is not specified whether the analyzed films were mixtures or single phases. The binding energy values and the FWHM for Bi 4f and O 2p peaks, found in the films deposited on Al_2O_3 and oxidized Si(100), are reported in

Table 3. XPS data of pure α- and β-Bi₂O₃ films grown on SiO₂/Si(100) and Al₂O₃.

	Bi 4f$_{7/2}$		O 1s			
Sample/phase	BE (eV)	FWHM	BE (eV)	FWHM	BE (eV)	FWHM
1/β	158.9	2.1	529.5	2.1	531.3	2.0
5/α	158.8	1.8	529.5	1.7	531.4	1.9
8/β	158.8	2.0	529.5	1.9	531.2	2.2
7/α	158.8	1.6	529.4	1.8	531.1	2.2

Table 3. The binding energy values (4f$_{7/2}$ component) are spread around a value of 158.8 eV and cannot be used to identify the crystalline phase. The reported data show instead a systematic increase in the FWHM of the Bi 4f peak on going from the α- to the β-Bi₂O₃ phase in the deposited films.

The greater values of the FWHMs in the case of the β phase can be explained in terms of the reported structure for β-Bi₂O₃.[11] This is a highly disordered phase as demonstrated by the XRD data, collected at room temperature, and by the thermodynamic data that show an increase in the entropy on passing from α- to β-Bi₂O₃.[12] It is therefore not unexpected that a higher disorder of the oxygen atoms around each bismuth center is responsible for the increase in the Bi 4f FWHM. The different electrical properties of these two phases can also be a possible cause of different charging effects on the surface, leading, in the case of the β phase, to an increase in the FWHMs of the photoelectronic peaks (see Table 3). The O 1s peak is found in all cases at about 529.5 eV. The basic character of these oxides is clearly deduced from the O 1s lineshape, which, as expected, is distorted towards higher binding energies. The higher binding energy component is due to the presence on the surface of oxygen atoms belonging to OH$^{\ominus}$, H₂O, and O₂.[13] A thermal treatment of the samples at about 400 °C for several minutes drastically reduces the high binding energy component of the O 1s peak. XPS depth profiles show a carbon content in the films lower than 1 % atomic fraction. Only adventitious carbon is present on the surface and can be easily sputtered away after a few minutes.

The thickness of the films deposited on Al₂O₃ was measured by a profilometer and was about 0.5 μm for both α- and β-Bi₂O₃ samples. The β-Bi₂O₃ films deposited on SiO₂/Si(100) were much thinner, with a thickness ranging from 0.05 to 0.06 μm. The α-Bi₂O₃ film deposited on the same substrate shows a very irregular coverage of the surface so that the thickness was determined by evaluating the height of the crystallites by AFM. The obtained value ranges from 1.0 to 1.2 μm.

Some qualitative considerations about the morphology of the film surface can be made from the observation of the AFM images. The micrographs corresponding to the α and β phases grown on surface-oxidized Si(100) and Al₂O₃ are reported in Figure 2. The films deposited on SiO₂/Si(100) show a completely different morphology in the two cases. In the case of the β sample a very fine texture is found. The film appears to be nanostructured with a particle size of about 0.11 μm. The coating follows the substrate irregularities. The α-Bi₂O₃ film shows a different morphology with
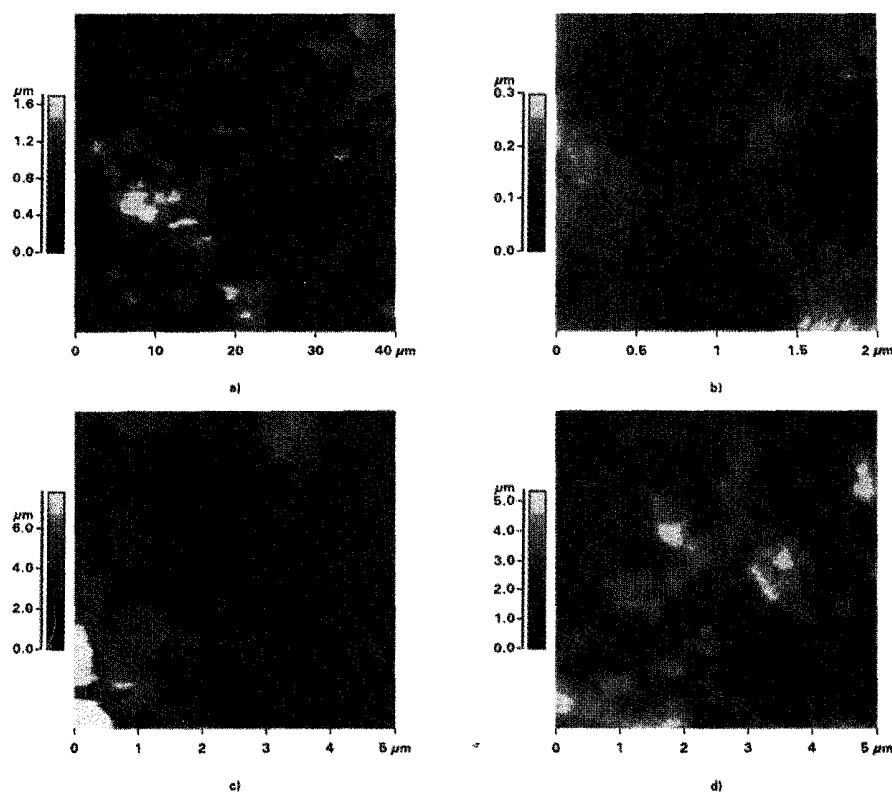

Fig. 2. AFM images of a) α-Bi₂O₃ on SiO₂/Si(100), b) β-Bi₂O₃ on SiO₂/Si(100), c) α-Bi₂O₃ on Al₂O₃, d) β-Bi₂O₃ on Al₂O₃.

much larger crystallite size (3 μm) and therefore the sampled area is also larger than in the case of β-Bi_2O_3 film. The surface is not covered uniformly, as can be seen in the micrograph: large spaces are found between the crystallites, corresponding to uncovered SiO_2 areas. The smaller particle size in the case of the β phase indicates that a higher number of nucleation sites are formed on the surface when the deposition parameters used are suitable for obtaining β-Bi_2O_3 films, that is, low flow rates. On the other hand, at high flow rates few nucleation sites are formed and the crystallites increase their size as long as the film grows. This indicates a preferential growth on the Bi_2O_3 crystallites with respect to the SiO_2 surface. When the Bi_2O_3 particle density is high (β phase with small crystallites) many nucleation sites are formed per unit time, the film grows uniformly and it is likely that in this way each Bi_2O_3 crystallite grows in the less thermodynamically stable phase. On Al_2O_3 the β phase is obtained at higher flow rates. In this case the film grows on the Al_2O_3 particles, showing a uniform coverage of the substrate. In the micrograph the Bi_2O_3 crystallites can be easily seen covering the much bigger Al_2O_3 particles. The α phase grows at lower flow rates and, as can be seen in the micrograph, the crystallite size is bigger than in the β phase. On alumina there is not a marked difference between Bi_2O_3 and Al_2O_3 nucleation sites due to the chemical similarity between the two oxides. Both oxides are partially ionic so that the electrostatic potential experienced by the Bi(III) ions on the Al_2O_3 and Bi_2O_3 particles is quite similar. Therefore, it seems plausible that when the flow rate is higher a large number of Bi_2O_3 nucleation sites is formed per unit time so that the crystallites once again grow in their less thermodynamically stable form and the β phase is thus favored.

The different electrical properties of Bi_2O_3 phases make this oxide, prepared as a thin film, an interesting material for gas sensing devices. These applications obviously require an easy and reproducible synthesis procedure which allows the phase composition of the films to be controlled. We have demonstrated that it is possible to deposit single and mixed phase Bi_2O_3 films by MOCVD. Simple variations of pressure and flow rate of the carrier gas (O_2) correspond to variations in the phase composition of the films so that it is virtually possible to obtain all the different phase compositions ranging from pure α- to pure β-Bi_2O_3 by choosing the proper pressure and flow rate combinations. We showed that strong differences are present in the IR spectra of α- and β-Bi_2O_3, so that it is possible to characterize very easily and quickly the phase composition of each sample by FTIR in the case of films deposited on SiO_2/Si(100). Some qualitative conclusions about the growth modality of the films on Al_2O_3 and SiO_2/Si(100) can be drawn from the AFM micrographs. Homogeneous films can be obtained on Al_2O_3 for both α and β phases while on surface-oxidized Si(100) only β-Bi_2O_3 and mixed phase Bi_2O_3 show a uniform coverage of the substrate, as demonstrated by the AFM images (the micrographs referring to

the mixed phase samples are not reproduced in the text). Aluminum oxide is therefore a more suitable substrate to grow uniform Bi_2O_3 thin films.

Experimental

Film deposition: The films were deposited in a tubular cold wall reactor using Bi(C_6H_5)$_3$ (Aldrich) as precursor. Oxygen was used as transport and reactive gas. The substrate temperature was kept in all cases at 420 °C by a resistively heated susceptor. The precursor was placed in a crucible inside the reactor tube and heated up. The tubing and valve system was heated to a temperature between 90 and 110 °C to avoid condensation of the precursor. The pressure was measured by a capacitance manometer and the gas flow was controlled by a mass flow controller. The growth conditions for the different samples are summarized in Tables 1 and 2.

The Si(100) wafers were first cleaned using a "wet etching" procedure [14] and then surface-oxidized in air at 850 °C for 2 h. The Al_2O_3 substrates (Spec.Tec A493) were ultrasonically degreased in warm trichloroethylene and successively rinsed in ethanol.

α- and β-Bi_2O_3 powder preparation: β-Bi_2O_3 was prepared by heat treatment of $Bi_2O_2(CO_3)$ at 380 °C in a Perkin Elmer TGS-2 thermobalance in order to control the stoichiometry of the reaction. A further heating of the yellow β-Bi_2O_3 powder to 650 °C for 10 min gave the pure α phase [15].

Instrumentation: Diffuse reflectance spectra of Bi_2O_3 powder samples were recorded on a Bruker IFS-66 spectrometer. The samples were diluted in KBr. The IR spectra of the films, deposited on surface oxidized Si(100), were recorded in transmittance mode on the same instrument.

A Perkin Elmer Φ 5600ci spectrometer with standard AlKα radiation (1486.6 eV) was used for the XPS analyses. The working pressure was less than 1.8×10^{-9} mbar. The spectrometer was calibrated by assuming the binding energy (BE) of the Au $4f_{7/2}$ line at 83.9 eV with respect to the Fermi level. As an internal reference for the peak positions the C 1s peak of hydrocarbon contamination was assumed at 284.8 eV. The standard deviation in the BE values of the XPS lines is 0.10 eV. After a Shirley-type background subtraction, the raw spectra were fitted using a nonlinear least-square fitting program adopting Gaussian–Lorentzian peak shapes for all the peaks. The atomic compositions were evaluated using sensitivity factors as provided by Φ V5.4A software. Depth profiles were carried out by $Ar^{\oplus}$ sputtering at 2.5 keV, 0.4 mA cm^{-2} beam current density with an argon partial pressure of 5×10^{-8} mbar.

AFM data were taken using a Park Autoprobe CP instrument in contact mode. No image processing was carried out on the image screen.

X-ray diffraction measurements were performed on a Philips MPD 1880 powder diffractometer with monochromatized CuKα radiation in the Bragg–Brentano parafocusing geometry. The sample holder did not contribute to the diffraction patterns.

[1] J. George, B. Pradeep, K. S. Joseph, *Thin Solid Films* **1987**, *148*, 181
[2] H. A. Harwig, A. G. Gerards, *J. Solid State Chem.* **1978**, *26*, 265.
[3] T. Sekiya, Y. Torii, *Mater. Res. Bull.* **1984**, *19*, 885.
[4] A. D. Berry, R. T. Holm, M. Fatemi, D. K. Gaskill, *J. Mater. Res.* **1990**, *5*, 1169. M. Miyajima, R. Muhammet, M. Okada, *J. Chem. Soc. Jpn.* **1991**, *10*, 1373.
[5] a) L. Seguin, M. Figlarz, R. Cavagnat, J. C. Lassegues, *Spectrochim. Acta A* **1995**, *51*, 1323. b) F. D. Hardcastle, I. E. Wachs, *J. Phys. Chem.* **1991**, *95*, 10763.
[6] a) K. Matsuo, K. Nakano, *Appl. Surf. Sci.* **1989**, *41/42*, 53. b) F. M. Ismail, E. E. Elsherefy, *Egypt. J. Chem.* **1985**, *28*, 539. c) N. T. McDevitt, W. L. Baun, *Spectrochim. Acta* **1964**, *20*, 799. d) S. N. Narang, N. G. Patel, V. B. Kartha, *J. Mol. Struct.* **1994**, *327*, 221. e) N. M. Sammes, G. Tompsett, A. M. Cartner, *J. Mater. Sci.* **1995**, *30*, 4299.
[7] J. W. Medernach, R. L. Snyder, *J. Am. Ceram. Soc.* **1978**, *61*, 494.
[8] Pattern 27-50 on JCPDS-ICDD (Joint Committee on Powder Diffraction Standards–International Center for Diffraction Data), **1993**.
[9] Pattern 41-1449 on JCPDS-ICDD (Joint Committee on Powder Diffraction Standards–International Center for Diffraction Data), **1993**.
[10] a) V. S. Dharmadhikari, S. R. Sainkar, S. Badrinarayan, A. Goswami, *J. Electron Spectrosc. Relat. Phenom.* **1982**, *25*, 181. b) T. P. Debies, J. W. Rabalais, *Chem. Phys.* **1977**, *20*, 277.
[11] S. K. Blower, C. Greaves, *Acta Crystallogr. C* **1988**, *44*, 587.